Proceedings of the World Congress on Engineering 2007 Vol II
WCE 2007, July 2 - 4, 2007, London, U.K.

Anisotropic Imaging Of Tumours Using Elastic Wave Signals

Clifford J. Nolan & Niall Ryan *

Abstract—**In this short paper we show how one may extract elastic properties of materials by probing it with elastic waves and processing the signal that returns (i.e. the scattered waves) in an appropriate way. In particular, we present a linearized inversion scheme to estimate the high–frequency, anisotropic components of the elastic tensor and density (the elastic moduli) in human tissue. For a given configuration source and receiver transducers, we show what combinations of moduli can be determined. Conversely, to estimate moduli in a specified region of the tissue, we derive an algorithm that searches for an optimal configuration of transducer pairs which best resolves the moduli. The ultimate goal of this work is application to biomedical imaging for early detection of tumours.**

Keywords: Biomedical Imaging, Signal Processing, Multistatic scattering, Waves, Anisotropic media

1 Introduction

A linear elastic material is characterized by its density and Hooke's tensor fields, henceforth referred to as elastic moduli. Hooke's tensor has rank 4 and relates stress to strain linearly. Symmetry considerations yield 21 independent components of the Hooke's tensor c, so that there are 22 moduli in general. Specialization to specific elastic materials yields less components, e.g., isotropic materials have 3 moduli; the Lamé parameters and density. We lump the density and Hooke's tensor fields together and refer to them as *elastic moduli* for brevity. We are especially interested in anisotropic materials where the speed of elastic wave propagation is direction–dependent.

We consider the elastic moduli fields $c := \{c_i : i = 1, \ldots, 22\}$ as a superposition of *known* background fields c_0 and *unknown* perturbations δc, which vary rapidly compared to wavelength scale. We linearize the equations of elasticity about c_0. The equations of motion for the perturbed displacement field δu satisfy the equations of linear elasticity with a source term involving the background displacement u_0 and δc. The *scattering operator* $\mathcal{F} : \delta c(x) \to \delta u(s, r, t)$ maps the perturbation δc to the solution δu of the perturbed equations of motion. Here x is a scattering location in the tissue and $\delta u(s, r, t)$ is the scattered field due to a point source located at s, measured at receiver location r at time t.

Statement of main results. It is possible to construct an ensemble of *independent* experiments involving various mode converted waves, so that the scattering operator associated to the ensemble is invertible. This leads to an inversion algorithm for recovery of the elastic moduli. Such information can be used to directly infer the presence or absence of a tumour in human tissue. Furthermore, for a given locale in the tissue, one may optimize the choice of ensemble so that the inversion procedure is optimally stable there, i.e., the linear systems involved in inversion are optimally-conditioned.

Our work is an extension of that in [2], [3]. The latter papers use a combination backprojection and statistical analysis to estimate the elastic moduli. In this paper, we avoid the statistical element and instead show how to estimate the moduli in a deterministic and stable (with respect to noise) manner. It can also be viewed as an extension of [1] which shows how to estimate the Lamé parameters in isotropic elasticity.

We have ignored the complications caused by wave focusing (caustics). Some of these complications can be dealt with using techniques developed in [6]. We also remark that the results in this paper are only valid provided that anisotropic waves in very special directions are filtered out; namely those travelling in the optic axis direction. This is because the background propagating field is much more complicated than the simpler approach taken here (see [7], [8] for more details).

2 Forward Modeling

2.1 Equations of motion

The i–th component u_i of the deformation field u of an elastic material with density ρ and Hooke's tensor c_{ijkl} satisfies [5]

$$\rho \frac{\partial^2 u_i}{\partial t^2} - (\, c_{ijkl} u_{k,l}), j = 0 \qquad (1)$$

*We acknowledge the support of Science Foundation Ireland in producing this paper. Contact Info: Department of Mathematics & Statistics, University of Limerick, Castletroy, Co. Limerick, Ireland. Email: Clifford.Nolan@ul.ie., Niall.Ryan@ul.ie. Tel. +353-61-202766.

where $(\cdot)_{,i}$ is shorthand for partial differentiation; $\partial_{x_i}(\cdot)$ and the index summation convention applies. We linearize about *a-priori known* background fields $\rho^0,\ c^0_{ijkl}$ and write

$$c_{ijkl} = c^0_{ijkl} + \delta c_{ijkl};\ \rho = \rho^0 + \delta\rho;\ u = u^0 + \delta u \qquad (2)$$

so that the perturbed field satisfies the formal linearized equation

$$\rho^0 \frac{\partial^2 \delta u_i}{\partial t^2} - (c^0_{ijkl}\delta u_{k,l}),j = -\delta\rho \frac{\partial^2 u^0_i}{\partial t^2} + (\delta c_{ijkl} u^0_{k,l}),j \quad (3)$$

2.2 The scattering operator

For simplicity, let us assume the background medium is isotropic (an assumption that can be relaxed). Suppose we measure a particular component of a scattered field due to a particular component of the incident field, and that there is no density perturbation. It can be shown [3] that the following is an approximate value for the scattered field due to a perturbation δc in the Hooke's tensor:

$$\delta u(s,r,t) = \int dx'\ \xi(s,x')\xi(r,x')A(s,r,x')$$
$$w^T(s,r,x')\delta c(x')\ \delta''(t-\tau(s,x)-\tau(r,x)) \qquad (4)$$

with a similar formula holding when there is a density perturbation. The formula is for a single mode propagating and a single mode reflecting and ξ is a scalar function representing just one component of a polarization vector. The function $\tau(s,x)$ is the travel time from s to x and a similar definition for $\tau(r,x)$. The travel time functions depend on the mode of propagation in each case. The function A is related to geometrical optics amplitudes, which describe how energy is spread over the propagating wavefront. The function δ'' is the second derivative of the Dirac-delta function. We have written the components of δc as a column vector and the weight w^T as a row vector of the same dimension. The function $w \in R^N,\ N \leq 21$ is a kinematical weighting on the elastic perturbation $\delta c \in R^N$ and is called the *radiation pattern*. Here, we assume an anisotropic model has N elastic parameters that characterize it. More generally, the scattered signal is a sum of terms (4) for the various incident and reflected modes. However, it is possible to isolate data described in (4) by taking appropriate projections of the actual data; these projections annihilate unwanted polarization modes.

We are also assuming that the incident waves only scatters once with a scatterer before returning to the sensor for measurement. It is possible to incorporate multiple scattering between unknown scatterers and known environmental scatterers (see [11] for more details).

Let X represent a three dimensional region within the tissue under examination. We assume that we can filter reflections from the boundary B (locally defined by the equation $x_3 = 0$ say) of X. Partition the B into N distinct bounded region pairs $\Sigma^k_{s,r} \subset B \times B, k = 1, \ldots N$. We use coordinates $(s, r(s), t) \in \Sigma^k_{s,r} \times (0,T),\ k = 1, \ldots, N$ to describe N source and receiver regions. Thus, r is a function $r(s)$ of s and $(s, r(s))$ simultaneously refers to N pairs of sources and receivers in $\bigcup_k \Sigma^k_{s,r}$ varying smoothly with s. There are many other options available to us here with regard to partitioning the data space but we chose the one above to simplify this exposition. For each region $\Sigma^k_{s,r}$, we cam employ a separate weighting vector w_k.

Define the k–th component of the linearized scattering operator $\mathcal{F}$ by formula (4) with w replaced by w_k. Here k refers to experiment k which describes a fixed $\Sigma^k_{s,r}$ and a fixed mode of scattering (i.e. specified polarization components for the incident reflected wave). We form the matrix $W^T(s,r,x')$ whose k–th row is $w^T_k(s,r,x')$.

For the next definition, we need to define the diagonal matrix $\triangle(e^{i\omega(t-\tau(s,x)-\tau(r,x))})$ whose i-th diagonal entry is $e^{i\omega(t-\tau_k(s,x)-\tau_k(r(s),x))}$, where $\tau_k(s,x), \tau_k(r(s),x)$ are the traveltime functions for the incident and reflected mode in experiment k. Define the *ensemble scattering operator* $\mathcal{F}$ associated to the various experiments as

$$\mathcal{F}\cdot\delta c(s,t) := \int d\omega dx' \triangle(e^{i\omega(t-\tau(s,x)-\tau(r(s),x))})$$
$$W^T(s,r(s),x')\ \delta c(x') \qquad (5)$$

where we have absorbed the polarization functions ξ and amplitudes A into the the weighting matrix W^T. If d is the recorded data ensemble, then

$$d(s,t) = \mathcal{F}\cdot\delta c(s,t) \qquad (6)$$

3 Linearized Inversion

Let $g(s,x) \in R^{N\times N}$ be a smooth matrix–valued function to be determined. We form an image via backprojection:

$$Image(x) = \int dsdtd\omega' g(s,x)$$
$$\triangle(e^{-i\omega'(t-\tau(s,x)-\tau(r,x))})\ d(s,r,t) \qquad (7)$$

which is a weighted adjoint of $\mathcal{F}$ applied to the data. In this and the expression that follow, r is to be interpreted as the function $r(s)$.

If we substitute (5) into this for the data, after carrying out a stationary phase calculation [13], we obtain an expression

$$Image(x) \approx \int d\omega ds dx'\ g(s,x)W(s,r,x')\ \delta c(x')$$
$$\triangle(e^{i\omega(\tau(s,x)+\tau(r,x)-\tau(s,x')-\tau(r,x'))}) \qquad (8)$$

We use Taylor's integral remainder theorem to write $\omega(\tau(s,x) + \tau(r,x) - \tau(s,x') - \tau(r,x')) = (x - x')\cdot$

$(\omega f(s,r,x',x))$, where f is remainder in Taylor's theorem [12]. Because of the factor $(x-x')$ that this introduces into the phase, the stationary phase theorem [13] tells us that most of the contribution to the image signal comes from $x = x'$. So if δc is varying rapidly at x' then the same will be true for the $Image$ function. This is the basis of our signal processing (imaging algorithm).

If instead of using a single set of sources s to parametrize the data ensemble, we had used N sets of source variables s (which complicates the notation), then we can make a change variable $\nu = \omega f(s,x',x)$ in (8) for each experiment, resulting in

$$Image(x) \approx \int dx' d\xi \; g_1(x',\xi) W_1^T(x',\xi) \\ \triangle(e^{i\omega'(x-x')\cdot\xi}) \; \delta c(x') \qquad (9)$$

where g_1, W_1^T are related to g, W^T via a stationary phase reduction. Provided that W^T can be arranged to have full rank, then, automatically W_1^T has full rank. Therefore, we choose g_1 as the inverse matrix of W_1^T multiplied by $(2\pi)^{-3}$, and we obtain

$$Image(x) \approx \int dx' \; \delta(x-x')\delta c(x') = \delta c(x) \qquad (10)$$

3.1 Rank of W^T in an isotropic background

We recall [3] the definition of the weight (suppressing geometric optics scalar multiplicands and polarisation factors that do not effect the rank) involved in a typical row of W^T,

$$w(s,r,x,\eta)_{ijkl} = \frac{1}{2}(a_{ij}(s,x,\eta)a_{kl}(r,x,\eta) + \\ a_{ij}(r,x,\eta)a_{kl}(s,x,\eta)) \qquad (11)$$

where

$$a_{ij}(s,x,\eta) \equiv \frac{1}{2}(\xi_i(s,x,\eta)\gamma_j(s,x,\eta) + \\ \xi_j(s,x,\eta)\gamma_i(s,x,\eta)), \qquad (12)$$

and $\gamma(s,x,\eta), \xi(s,x,\eta)$ are now described. Let γ be the slowness vector defined by

$$\gamma(s,x) := \nabla_x \tau(s,x) \qquad (13)$$

with a similar definition for $\gamma(r,x)$. With this definition, τ satisfies the Eikonal equation:

$$det\ (\rho^0 \delta_{ik} - c^0_{ijkl}\gamma_j\gamma_l) = 0. \qquad (14)$$

The (normalized) polarizations ξ are the corresponding eigenvectors and so satisfy

$$c^0_{ijkl}\gamma_j\gamma_l\xi_k = \rho^0\xi_i. \qquad (15)$$

The associated polarization vector ξ then is either one of the two orthonormal vectors to γ or else the unit vector parallel to γ depending on which slowness sheet we are considering i.e. which polarization mode is under consideration; quasi-P wave, quasi-SH wave or quasi-SV wave.

The tensor $w(s,r,x)_{ijkl}$ exhibits precisely the same symmetries as the elastic tensor c_{ijkl} itself does. We will show below that there are 21 independent components in the radiation tensor $w(\cdot,\cdot,\cdot)_{ijkl}$ for a quasi-P-P mode. Here, a quasi-P-P mode means that $\xi(s,x)$ is approximately parallel to $\gamma(s,x)$ and the same is true with s replaced by r. For quasi-P-S modes we have $\xi(s,x)$ approximately parallel to $\gamma(s,x)$ and $\xi(r,x,)$ is approximately perpendicular to $\gamma(r,x)$ (so that there are two modes here; quasi-P-SH and quasi-P-SV) . Furthermore, in the cases of quasi-P-S and quasi-S-P the number of independent members of $w(s,r,x)_{ijkl}$ is 20 while the number of independent members for the quasi-S-S mode is just 15.

It is possible to give an (lengthy) algebraic proof of the statements about the rank of W^T in the last paragraph. This would take up too much space in this short paper, and so instead, we will present numerical evidence of this in the next section. However, the algebraic proof is actually useful from a practical point of view because it shows us how to choose the regions $\Sigma^k_{s,r}$ so that the rank of W^T is optimally conditioned. We will present the full detail of these calculations elsewhere.

4 Numerical Results

Figure 1 shows a plot of W^T (no density perturbation) corresponding to δc varying rapidly across a surface whose normal has various orientations (dips), and only quasi-P-P mode conversions are present. One can plainly see that W^T has full rank from the triangular structure of the matrix, and non-zero entries along the diagonal. The corresponding plot of singular values for matrix W^T is displayed in figure 2. In the figure annotations, *polarisation mode* or *index* refer to an experiment index $k = 1, \ldots, N \leq 22$.

Figure 3 shows W^T (with density perturbation) and figure 4 shows the corresponding SVD. The caption in figure 4 refers to $N \times N$ matrices Γ and Ξ, which are the matrices whose rows are the various slowness γ_k and polarisation ξ_k vectors. In figure 3 there are several modes present in the experimental ensemble. The choice was determined by attempting to minimize the condition number of W^T via a Newton search over various locations of the source-receiver sets $\Sigma^k_{s,r}$. Also, we only considered experiments with a vertical dip. From these experiments, we extracted the sub-matrix W^T corresponding to a transversely isotropic medium. The results are shown in figure 5 and 6. Figure 5 shows the SVD (with density) and figure 6 shows the 5 rows of W^T (without density) which are clearly linearly independent. Finally, figures 6 and 7 show the corresponding modes and experiments that went into the ensemble of 5 experiments to resolve

the TI moduli perturbations.

From this brief suite of experiments, it is clear that we can extract various combinations of elastic moduli from the scattered wave signals. Moreover, this information is of a quantitative rather than qualitative nature, which is potentially very useful to the clinician in determine the nature of a tumour.

5 Conclusions

We have shown how to use various elastic waves to image tissue stiffness in an optimally stable manner. The results may be at odds with the readers prior expectations of only being able to recover linear combinations of elastic moduli. But the situation is different here, we are only recovering the singular components of the the moduli, responsible for scattering. We are not attempting to recover the background fields. It is the latter fields that one can only expect to recover linear combinations, using tomography-like experiments. The background fields are responsible for the kinematics and the perturbed fields are responsible for the scattering, so it is not that surprising that we are able to recover the elastic moduli perturbations.

References

[1] Beylkin, G. and Burridge, R., *Linearized Inverse Scattering Problem of Acoustics and Elasticity*, Wave Motion (12), pp.15-27, 1990.

[2] Bleistein, N. and De Hoop, M., *Generalized Radon transform inversions for reflectivity in anisotropic elastic media*, Inverse Problems, (13), pp. 669-690, 1997.

[3] Burridge, R, Miller, D, De Hoop, M. and Spencer, C., *Generalized Radon Transform/Amplitude Versus Angle (GRT/AVA) migration/inversion in anisotropic media*, SPIE (2301), pp.15-27, 1994.

[4] Duistermaat, J.J., *Fourier Integral Operators*, Birkhäuser, 1996.

[5] Helbig, K., *Foundations of anisotropy for exploration seismics*, Pergamon Press, 1994.

[6] Nolan, C.J., *Scattering in the presence of fold caustics*, SIAM J. App. Math. (61), pp. 659-672, 2000.

[7] Nolan, C.J., *Permittivity recovery from multiple characteristic electric waves*, Comm. P.D.E. (13), pp. 573-601, 1997.

[8] Nolan, and C.J., Uhlmann, G., *Parametrices for symmetric systems with multiplicity*, Wave Motion (44), pp. 231-247, 2007.

[9] Rakesh, *A linearized inverse problem for the wave equation*, SIAM J. App. Math. (62), pp. 448-461, 1988.

[10] Sait-Raymond, X., *Elementary introduction to the theory of pseudodifferential operators*, CRC Press, 1991.

[11] Nolan, C.J., Cheney, M., Dowling, T., and Gaburro, R., *Enhanced angular resolution from multiply scattered waves*, Inverse Problems (22), pp.1817-1834, 2006.

[12] Lang, S., *Real and functional analysis*, Third Ed., Springer Verlag, 1993.

[13] Hormander, L., *Linear partial differential operators I*, Springer Verlag, 1990.

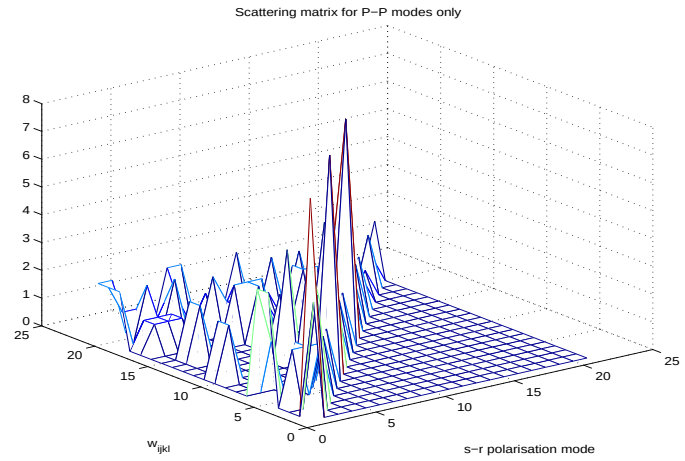

Figure 1: Scattering matrix for varying dips but all modes are P-P. The rank is 21 with condition number (2–norm) of 22.88.

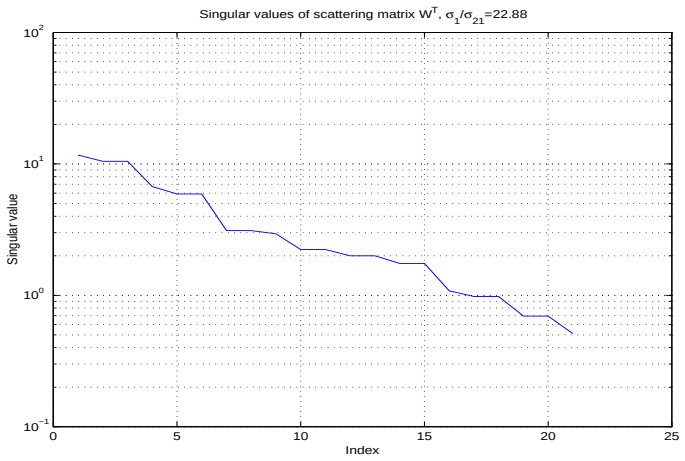

Figure 2: Singular values for P-P scattering.

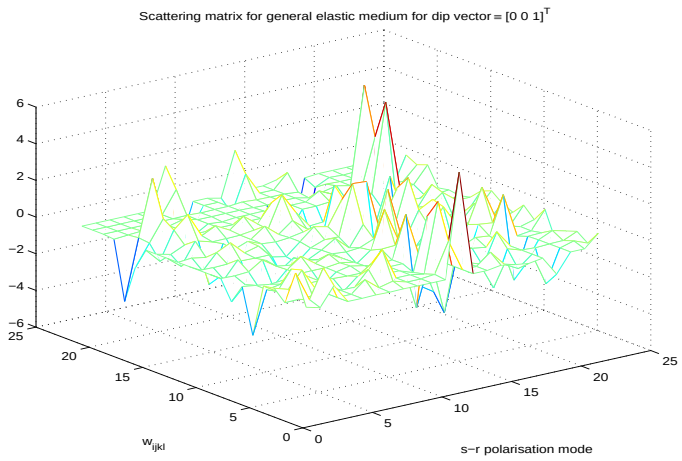

Figure 3: Scattering matrix W^T for vertical dips and multi–modal experiments. Density is included in this ensemble and condition number (2–norm) of 331.

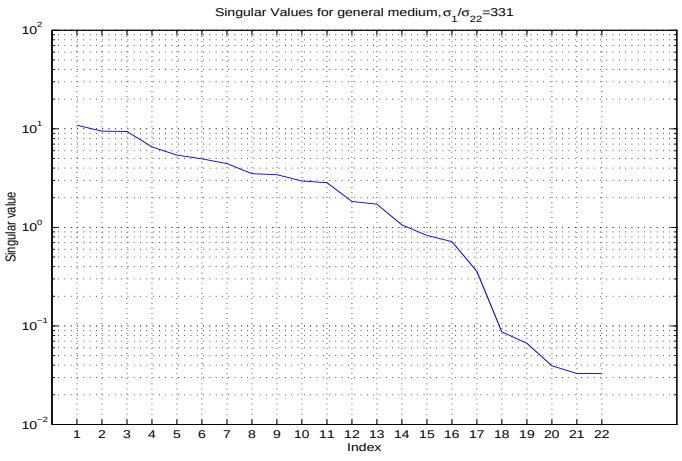

Figure 4: Singular values for modes and slownesses in Ξ, Γ associated to a vertical dip.

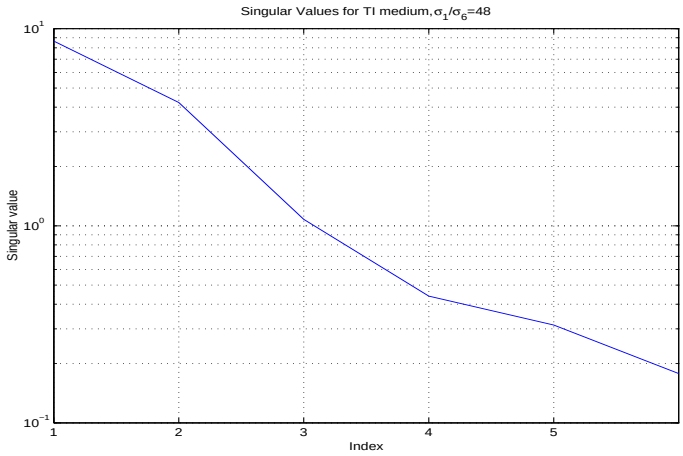

Figure 5: Singular values associated to vertical dip in a TI medium.

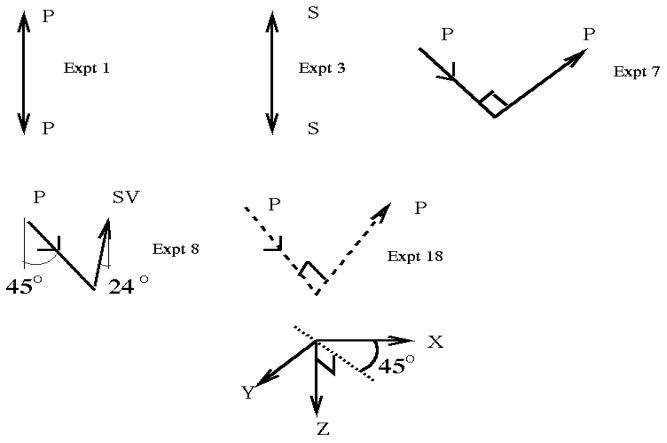

Figure 6: Five experiments that resolve the elastic parameters of a TI medium. Dashed lines indicate rays coming out of the page at a 45 degree angle. The ratio of the shear and compressional speeds was $1 : \sqrt{3}$.

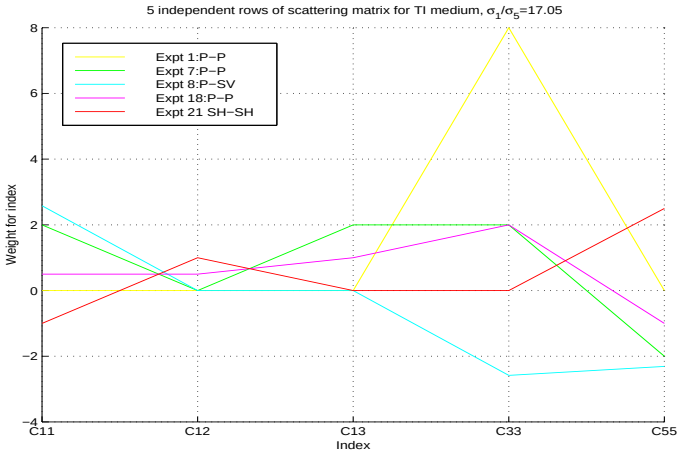

Figure 7: Five experiments of previous figure used to determine five TI moduli perturbations (excluding density).